Pergamon

Int. J. Heat Mass Transfer. Vol. 41, No. 11, pp. 1585–1599, 1998

Printed in Great Britain
0017-9310/98 $19.00+0.00

PII: S0017-9310(97)00278-0

Simultaneous determination of the thermal diffusivity of semiconductor lasers and resistance of their adhesive joints

V. LEPALUDIER and Y. SCUDELLER

Equipe de Thermophysique des Interfaces et des Microsystèmes, Laboratoire de Thermocinétique, URA CNRS 869, ISITEM, La Chantrerie, CP 3023, 44087 NANTES Cedex 03, France

(*Received* 6 *January* 1997 *and in final form* 26 *June* 1997)

Abstract—This paper describes a method to measure thermal diffusivity of laser diodes simultaneously with thermal resistance of their adhesive joints. The method is based on analysis of temperature variations of emitting regions caused by a quasi-continuous heat generation. A constant input power is applied in the laser diode during several seconds and switched off during some milliseconds. Temperature variations are detected during short sequences from about 10^{-6} up to 10^{-3} s. Temperatures are obtained from terminal voltage measurements resulting from injection of a small current. A steady state is reached during each large sequence and each short sequence can be then regarded as a transient state. Parameter identification uses a multidimensional heat diffusion model. Results have been obtained on a multistripe double heterostructure GaAs/GaAlAs laser diode owing ten emitting zones of 4 μm width. Thermal diffusivity of the substrate (N-GaAs) and thermal resistance of its adhesive joint have been identified. In addition, this method allows one to estimate steady state junction temperature and output optical power as a function of input current intensity. © 1998 Elsevier Science Ltd. All rights reserved.

1. INTRODUCTION

Temperature of semiconductor laser diodes has a strong influence on parameters such as threshold current, output optical power, wavelength of oscillating modes [1]. A lot of applications in communications, instrumentation, laser technologies, need a precise temperature control considering that structures, very compact in size, operate under unstationary regimes and with non-uniform heat generation [2–5]. Laser emission and heat generations are produced in very small volumes (a few cubic micrometers) into narrow regions of P–N junctions. Optical efficiencies being generally weak, volumic heat generation can reach more than 10^8 W/m^3.

Thermal characterization appears crucial, for integration and packaging design, to predict and test structures behaviour, specially under unstationary operating conditions. It consists in measuring temperatures (levels and temporal variations) as well as device thermophysical properties under stated conditions. The entire structure, composed of the laser diode attached on its submount, participates in heat diffusion. The thermal resistance of the joint, between the diode and its submount, may be considered as a thermal contact resistance R_c [6]. It characterizes the temperature drop across the bond which includes volumic defects. This definition may be applied in transient state if internal heat diffusion is very fast compared to structure one. Fatigue failures, inducing formation of defects such as cracks, causes important variations of R_c so its prediction cannot be accurate. Considering that R_c has a strong influence on temperature and transient behaviour, it has to be measured.

This paper describes a method to measure simultaneously thermal diffusivity of laser diodes and thermal resistance of their adhesive joints. In addition, maximum temperature and output optical power may be estimated. It is basically a transient method using laser diodes simultaneously as heat sources, dissipating in a quasi-continuous waveform, and temperature sensors. It can be viewed as a failure test.

2. DESCRIPTION OF STUDIED STRUCTURES

Conventional structures very compact in size (Fig. 1a) are considered. The semiconductor laser diode is connected on a conducting submount by a welded or an adhesive joint. Thicknesses are typically about 100 μm for the laser; a few millimetres for the submount and included between 5 to about 10 μm for the joint. The laser emission is produced when the laser diode is crossed by a current above threshold, from P to N regions. The emitting zone, very close to the PN junction, is less than 1 μm thick.

Studied devices are double heterostructure laser diodes, oxide isolated, grown by liquid-phase epitaxy, having several centred stripes (Fig. 1b). Each stripe is separated from each other by proton-isolated areas.

NOMENCLATURE

a, b, c	dimensions [m]
F	transfer function
I	heating current [A]
I_0	measurement current [A]
m	number of emitting zones
N	number of laser diode layers
p	complex variable
P	dissipated power [W]
P_i	input power [W]
P_o	optical power [W]
q	surface heat generation density
Q	volume heat generation density
R_c	thermal contact resistance
t	time [s]
T	temperature [K]
T_a	heat sink temperature [K]
T^*	reduced theoretical temperature
U	unit response [K/W]
V	voltage [V]
x, y, z	coordinates.

Greek symbols

α	thermal diffusivity [m^2/s]
η	optical efficiency
θ	temperature [°C]
θ_i	steady state junction temperature
θ^*	reduced experimental temperature
λ	thermal conductivity [W/m K].

Subscripts

i	laser diode layer
c	interface at the bottom of the laser
s	submount.

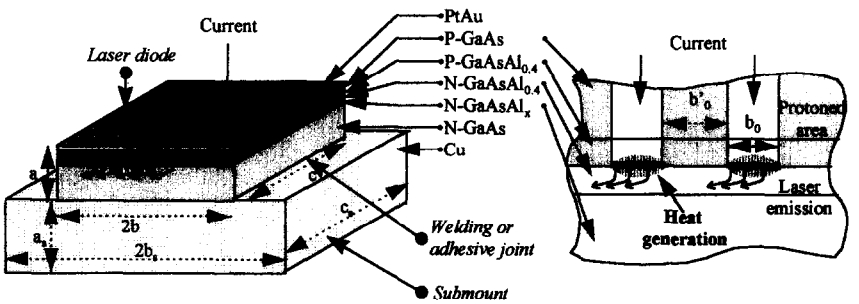

1.a : Description of the structure 1.b : Zoom at junctions

Fig. 1. GaAlAs/GaAs ten-stripes laser diode.

The output facets are passivated with Al_2O_3 coating. The active region of P-GaAs is bounded by $Ga_{0.6}Al_{0.4}As$ clad layers. Aluminium contents decrease refractive indexes, so these layers play a role of waveguide for the radiation. The capping layer P^+-GaAs is metallized with PtAu. Main dimensions are given in Table 1. The substrate (N-GaAs) represents more than 90% of the laser thickness. Thermophysical properties of each medium are given in Table 2 [3, 7]. The device is mounted P-side up.

If P_i denotes the input power and P_0 the optical output power, then the dissipated power P is:

$$P = P_i - P_o \tag{1}$$

P represents up to 80% of P_i. Heat generations are

Table 1. Laser diode and submount dimensions (μm)

Laser diode width	$2b$	350	Submount width	$2b_s$	1240
Cavity length	c	620	Submount length	c_s	740
Laser diode thickness	a	88	Submount thickness	a_s	300
Heat sources width	b_0	4	Protoned areas width	b'_0	6

Table 2. Thermophysical properties of laser diode layers and submount

Layer	Material	a_i (μm)	Doping (cm^{-3})	λ_i (W/m K)	α_i (m^2/s)
1	PtAu	2	—	300	1.25×10^{-4}
2	P^+-GaAs	1	10^{19}	45	2.5×10^{-5}
3	P-$GaAsAl_{0.4}$	2	5×10^{17}	11	0.6×10^{-5}
4	N-$GaAsAl_{0.4}$	1.5	10^{18}	11	0.6×10^{-5}
5	N-$GaAsAl_x(0<x<0.4)$	1.5	10^{18}	15	0.8×10^{-5}
6	N-GaAs	80	2×10^{18}	45	2.5×10^{-5}
Submount	Cu	300	—	380	1.16×10^{-4}

non-uniformly distributed. The total power is given by:

$$P=\int_V Q(M)\,\mathrm{d}V \tag{2}$$

$Q(M)$ is the volumic heat generation at each point M of the laser diode. Heat sources can be assumed to be mainly located at the P–N junction on each emitting zone, photon absorption outside emitting zones occurring essentially below threshold [8–10]. Consequently, all heat sources can be represented as a heat flux density $q(M)$ generated at the P–N junction.

3. PRINCIPLE OF THE METHOD

The method is suitable for most semiconductor laser devices. Basically, it consists in generating controlled variations of input power P_i by imposing an unstationary current I to the laser diode. Injection of current produces strong variations of the total dissipated power P and causes temperature shifts. Analysis of temporal variations of temperature, measured inside the emitting regions, allows one to identify, by comparison with a theoretical model, thermophysical properties of the structure.

Temperature is measured by detection of a differential voltage δV between both sides of the laser diode (regions P and N) when a low current I_0 ($I_0 \ll I$) is applied. So, the current is switched from I (heating current) to I_0 (measurement current). Heat generation is only produced when the current I is applied and equal zero for the current I_0. Temperature of each active zone of a multistripe laser diode is not absolutely the same. Temperature measurement requires a calibration in which differential voltage δV is plotted versus junction temperature under the current I_0. Measured temperature, called junction temperature $\theta(t)$, appears as a mean value of temperature distribution of all emitting zones.

Many temporal forms can be used for P such as a single pulse (length equal to Δt) or a succession of pulses. They are capable to provide a lot of thermophysical properties at various depths of the structure. Measured properties depend on waveforms and time domain analyzed. In this paper, a quasi-continuous waveform is considered for P, that is to say a succession of very large pulses (duration Δt) of a constant power (Fig. 2). The temperature measurement, taking place between two pulses, has a very short duration Δt_0 in comparison with Δt. Δt has to be chosen in order that a steady state is reached during it. In these conditions, only a narrow depth of the structure is cooled during Δt_0 because of its short-live (a few milliseconds). The consequence is that each temperature measurement phase appears as a transient state.

Transient heat diffusion occurs typically from about 10^{-6} to a few 10^{-3} s. The structure being basically an heterogeneous medium, each time scale transient temperature is run by thermal properties of thin layers during a few 10^{-6} s, the thermal diffusivity of the substrate after a few 10^{-5} s, the thermal contact resistance after 10^{-3} s.

3.1. *Identification of substrate thermal diffusivity and thermal resistance of its adhesive joint from a quasi-continuous waveform*

As P is dissipated as a constant rate (P is independent of time) until the steady state is reached, then, the temperature distribution of the structure is $\theta_i(M)$. At $t=0$, P is suddenly switched off. Consequently, the temperature distribution $\theta(M,t)$, initially being equal to $\theta_i(M)$, decreases as a function of time and leads, for long time values, to a uniform temperature equal to the ambient one. Particularly, the mean temperature measured along the active junctions $\theta(t)$ may be deduced from the following relation:

$$\theta(t)=\theta_i-P\cdot U(t) \tag{3}$$

in which U is the temperature rise due to a unit step of dissipated power, the structure being initially at a uniform temperature equal to 0. U is the unit response of the structure and has a dimension of K/W. This relation is strictly valid if thermophysical properties do not depend on temperature. It can be used in all cases for small temperature differences between θ and θ_i. It has to be noticed that U is a function of the thermophysical properties but depends also on heat sources distribution inside the laser diode.

Measurement of $\theta(t)$ is done at any time, but is

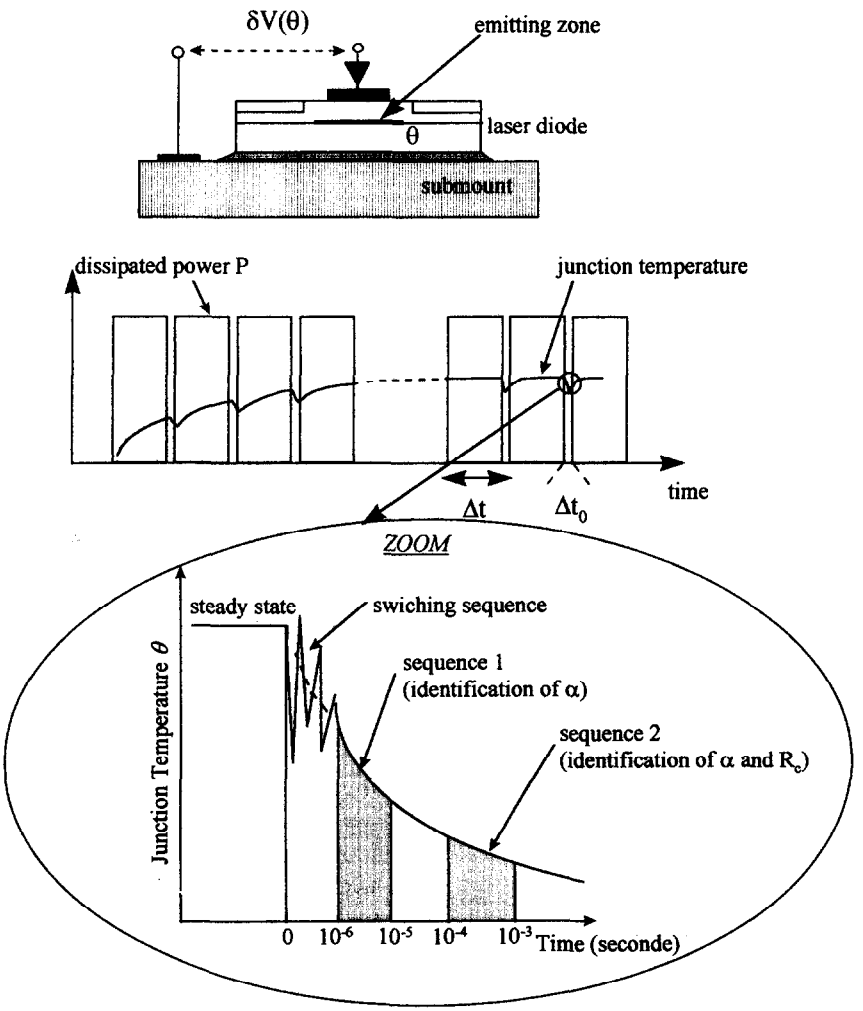

Fig. 2. Principle of the method—identification sequences of α and R_c.

strictly impossible at $t = 0$ because I_0 cannot be reached instantaneously. In addition, P is not known because P_0 is difficult to measure accurately (relation (1)). In order to free ourselves of the initial conditions (θ_i, P) which are usually unknown parameters, estimation of thermophysical properties is proceeded on a reduced temperature θ^*, defined as a fraction of two temperature differences, over a sequence $[t_0, t_0+\tau]$:

$$\theta^* = \frac{\theta(t_0)-\theta(t)}{\theta(t_0)-\theta(t+\tau)} \tag{4}$$

The time t is included between t_0 and $t_0+\tau$. t_0 is the start of the sequence, and τ its duration. The position of the sequence $[t_0, t_0+\tau]$ is determined considering the sensitivity of θ^* towards the whole parameters which is possible to identify. Basically, identification is achieved comparing the reduced experimental temperature θ^* with the theoretical one T^*, defined in the same way as θ^*. Considering the relation (2), the theoretical equivalence of θ^* given by equation (3) and called T^*, is expressed as:

$$T^* = \frac{U(t_0)-U(t)}{U(t_0)-U(t+\tau)} \tag{5}$$

U is obtained with a multidimensional heat diffusion model, in which the whole parameters β constitute the inlet variables. In practice, the identification consists in fitting the unknown parameters β in the calculation of T^*, in order to minimize the quadratic criterion defined by:

$$J = \sum_{k=0}^{n} \|\theta_{t=k_k^*} - T_{t=t_k^*}\|^2 \tag{6}$$

n is the number of experimental data in the identification sequence.

Two main identification sequences appear for most lasers. In the first one (typically 10^{-5}, 10^{-4} s), substrate thermal diffusivity α is the only parameter determining variations of θ^*, this first sequence corresponds to time where cooling down has not yet reached the joint. In the second one (typically 10^{-3} s), θ^* becomes also sensitive to the thermal resistance R_c

of the joint. So, it becomes possible to extract R_c from the second sequence, α being given from the first one (Fig. 2).

3.2. *Estimation of the steady state conditions from a quasi-continuous waveform*

Measurement of $\theta(t)$ is not possible at $t = 0$, so estimation of θ_i has to be achieved from an extrapolation of the junction temperature evolution $\theta(t)$. According to the relation (3), it needs to add to $\theta(t)$ a temperature rise $\delta\theta$ ($\delta\theta = P \cdot U(t)$). $\delta\theta$ is estimated from the heat diffusion model according to the fact that thermal diffusivity α and resistance of the joint R_c have been previously identified. Considering equation (3) at two moments t_0 and t in the very first times of the cooling down, it leads to θ_i depending only on U and θ:

$$\theta_i = \frac{\theta(t_0) \cdot U(t) - \theta(t) \cdot U(t_0)}{U(t) - U(t_0)} \tag{7}$$

In addition, an estimation of heat generation rate can be achieved:

$$P = \frac{\theta(t_0) - \theta(t)}{U(t) - U(t_0)} \tag{8}$$

The optical efficiency can be deduced from equation (8) and the measurement of P_i:

$$\eta = \frac{P_i - P}{P_i} \tag{9}$$

4. HEAT DIFFUSION MODEL

Parameter identification requires the calculation of the theoretical response $U(M, t)$ for the entire structure. The heat diffusion model assumes that heat sources are uniformly generated along the cavity inside each emitting zone–PN junction (Fig. 3). Each heat source is considered as a very thin stripe. The heat generation rate density q, generated at the junction, is a function of y-axis. Considering that $P = 1$ W, q has to satisfy the relation:

$$c \int_0^b q(y)\,dy = 1 \tag{10}$$

Considering the very high thermal conductivity of the submount, flux density $q_c(t)$ at interface joint–submount is assumed to be uniform. So, a mean contact temperature T_c is considered at this interface. Heat generation rate is uniform along the cavity, so temperature distribution in the laser diode is two-dimensional, depending on x and y axes only. But, submount being longer than laser diode ($b_c > b$), temperature distribution in the submount is considered as tridimensional. At a depth $x = a_c$ from the joint, temperature is taken equal to zero. The heterogeneous feature of the structure is taken into account. $N = 6$ layers are considered for the laser (see Tables 1 and 2).

With x and y, respectively, perpendicular and parallel axis to layers, conduction system in each laser diode layer i is written:

$$\lambda_x^i \frac{\partial^2 U^i}{\partial x^2} + \lambda_y^i \frac{\partial^2 U^i}{\partial y^2} = c_i \rho_i \frac{\partial U^i}{\partial t} \tag{11a}$$

$$y = 0 \quad \frac{\partial U^i}{\partial y} = 0 \tag{11b}$$

and $y = b$

$$x_1 = 0 \quad \frac{\partial U^1}{\partial x_1} = 0 \tag{11c}$$

$$x_i = 0 \quad \begin{cases} U^i(x_i = 0) = U^{i-1}(x_{i-1} = a_{i-1}) \\ \lambda_x^i \left.\dfrac{\partial U^i}{\partial x_i}\right|_{x_i = 0} = \lambda_x^{i-1} \left.\dfrac{\partial U^{i-1}}{\partial x_{i-1}}\right|_{x_{i-1} = a_{i-1}} \end{cases} \tag{11d}$$

$$x_i = a_i \quad \begin{cases} U^i(x_i = a_i) = U^{i+1}(x_{i+1} = 0) \\ \lambda_x^i \left.\dfrac{\partial U^i}{\partial x_i}\right|_{x_i = a_i} = \lambda_x^{i+1} \left.\dfrac{\partial U^{i+1}}{\partial x_{i+1}}\right|_{x_{i+1} = 0} \end{cases} \tag{11e}$$

At the junction between the layer j and $(j+1)$:

$x_{j+1} = 0$

$$\begin{cases} U^{j+1}(x_{j+1} = 0) = U^j(x_j = a_j) \\ -\lambda_x^{i+1} \left.\dfrac{\partial U^{j+1}}{\partial x_{j+1}}\right|_{xj+1=0} = -\lambda_x^j \left.\dfrac{\partial U^j}{\partial x_j}\right|_{x_j = a_j} + q(y) \end{cases} \tag{11f}$$

At laser–joint interface:

$$x_N = a_N \quad U^N = T_c(t) + R_c q_c(t) \tag{11g}$$

$$t = 0 \quad U^i = 0 \tag{11h}$$

And, in the submount:

$$\nabla T - \frac{1}{\alpha} \frac{\partial T}{\partial t} = 0 \tag{12a}$$

$$y = 0 \quad \frac{\partial T}{\partial y} = 0 \tag{12b}$$

and $y = b_s$

$$z = 0 \quad \frac{\partial T}{\partial z} = 0 \tag{12c}$$

and $z = c_s$

$$x = 0 \quad -\lambda_s \frac{\partial T}{\partial x} = q_c(t) \text{ if } 0 < y < b \text{ and } 0 < z < c$$

$$-\lambda_s \frac{\partial T}{\partial x} = 0 \quad \text{elsewhere} \tag{12d}$$

$$x = a_s \quad T = 0 \tag{12e}$$

$$t = 0 \quad T = 0 \tag{12f}$$

Determination of temperature field is based on integral transforms technique [11]. A Laplace transform

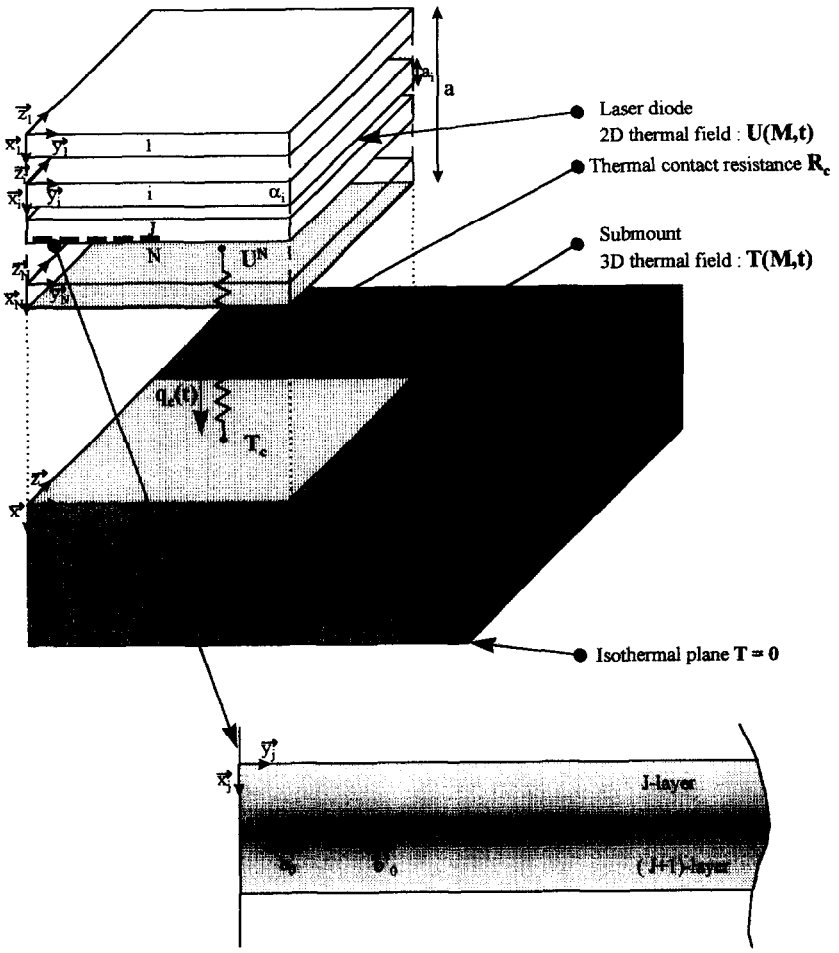

Fig. 3. Structure details and separation method.

equations (13) and (14) is applied on systems (11) and (12):

$$\bar{U}^i(M,p) = \int_0^\infty U(M,t)\exp(-pt)\,dt \qquad (13)$$

$$\bar{T}(M,p) = \int_0^\infty T(M,t)\exp(-pt)\,dt \qquad (14)$$

p is a complex variable.

If a mean temperature T_c is considered at interface joint–submount, then systems (11) and (12) can be solved separately.

Solution of equation (12) is obtained from a double finite fourier transform:

$$\tilde{\bar{T}}(x,\beta_n,\gamma_q,p) = \int_0^{b_s}\int_0^{c_s} \bar{T}(x,y,z,p)\cos(\beta_n y) \times \cos(\gamma_q z)\,dy\,dz \qquad (15)$$

with $\beta_n = (n\pi/b_s)$ and $\gamma_q = (q\pi/c_s)$.

Temperature field of the submount is then given by:

$$\bar{T} = \frac{\tilde{\bar{T}}_{n=0,q=0}}{b_s} + \frac{2}{b}\sum_{n=1}^{\infty}\tilde{\bar{T}}_{n,q=0}\cos\left(\frac{n\pi y}{b_s}\right) + \frac{2}{c}\sum_{q=1}^{\infty}\tilde{\bar{T}}_{n=0,q}\cos\left(\frac{q\pi z}{c_s}\right) + \frac{4}{b\cdot c}\sum_{n=1}^{\infty}\sum_{q=1}^{\infty}\tilde{\bar{T}}_{n,m}\cos\left(\frac{n\pi y}{b_s}\right)\cos\left(\frac{q\pi z}{c_s}\right) \qquad (16)$$

It leads to a relation linking the heat flux q_c, with the mean temperature rise T_c:

$$\bar{T}_c = \bar{F}\cdot\bar{q}_c \qquad (17)$$

$F(p)$ is a transfer function depending on geometry and thermal properties of submount, which has the following expression:

$$\bar{F} = \frac{1}{\lambda} \cdot \left\{ \frac{bc}{b_s c_s} \frac{\text{th}(\Gamma_{0,0} a_s)}{\Gamma_{0,0}} + 2 \frac{b_s c}{b c_s} \sum_{n=1}^{\infty} \frac{\text{th}(\Gamma_{n,0} a_s)}{\Gamma_{n,0}} A_{n,0} + 2 \frac{b c_s}{b_s c} \sum_{q=1}^{\infty} \frac{\text{th}(\Gamma_{0,q} a_s)}{\Gamma_{0,q}} A_{0,q} + 4 \frac{b_s c_s}{bc} \sum_{n=1}^{\infty} \sum_{q=1}^{\infty} \frac{\text{th}(\Gamma_{n,q} a_s)}{\Gamma_{n,q}} A_{n,q} \right\} \quad (18)$$

where

$$\Gamma_{n,q}^2 = \frac{n^2\pi^2}{b^2} + \frac{q^2\pi^2}{c^2} + \frac{p}{\alpha} \quad \text{and}$$

$$A_{n,q} = \frac{\sin^2\left(n\pi \frac{b}{b_s}\right)}{n^2\pi^2} \frac{\sin^2\left(q\pi \frac{c}{c_s}\right)}{q^2\pi^2}$$

If relation (17) is incorporated into relation (11g), a third kind condition of is obtained at $x_N = a_N$ in Laplace space:

$$-\lambda^N \left(\frac{\partial \bar{U}^N}{\partial x_N} \right)_{x_N = a_N} = \frac{\bar{U}^N}{\bar{F} + R_c} \quad (19)$$

To solve equation (11), a finite Fourier transfer equation (20) is applied to get a system of ordinary differential equations depending on the space variable x:

$$\tilde{\bar{U}}^i(x_i, p, \alpha_m) = \int_0^b \bar{U}^i(x_i, y, p) \cos(\alpha_m y)\, dy \quad (20)$$

with $\alpha_m = (m\pi/b)$.

Temperatures and fluxes are determined at each interface, using matrix formulation (Appendix) [12]. The real expressions are obtained, first by a numerical Laplace inversion–Gaver algorithm [13], and the inverse Fourier Transform:

$$\bar{U} = \frac{\tilde{\bar{U}}_{m=0}}{b} + \frac{2}{b} \sum_{m=1}^{\infty} \tilde{\bar{U}}_n \cos\left(\frac{m \cdot \pi \cdot y}{b}\right) \quad (21)$$

Junction temperature profiles are obtained in a short time. The method is particularly convenient to a sensitivity study. It must be noticed that the steady state distribution $\theta_i(M)$ can be calculated directly from $\bar{U}(\theta_i = P \cdot \bar{U}(M, p \to 0))$.

5. THEORETICAL ANALYSIS

Figure 4 presents temperature fields $\theta(x, y, t)$ inside a ten stripe laser diode before and after switching, at $t = 0$, 2 and 500 μs. At $t = 0$ (steady state), overheating appears very closed to junctions. Major temperature rise occurs in a very narrow region of the N-GaAs substrate and particularly into the clad layer N-GaAlAs which undergoes a quarter of the falling and represents less than 4% of the substrate thickness. The metallization has a strong influence on steady state temperature distribution. Increasing of its thickness reduces the mean temperature and the temperature variations along the junction (Fig. 5).

After $t = 2$ μs, the transient temperature variation of a multistripe laser diode is equivalent to a diode having a stripe of B_0 width (Fig. 6). This situation is due to the fact that this period corresponds approximately to establishment of microscale constriction where heat flux spreads out from b_0 to B_0/m, m denoting the number of emitting zone. At about $t = 500$ microseconds, temperature distributions become monodimensional. It corresponds to establishment time of macroscale constriction where heat flux spreads out from B_0 to b. Thus, two scales of constriction occur during heat diffusion. The first one, at macroscale, determines the mean temperature along B_0. The second one, at small sources scale, determines the rise in temperature from this mean temperature and characterizes the non-uniformity of heat generation along B_0.

Normalized sensitivity coefficients S_β on the various parameters, denoted by β, have been calculated to find the position of identification sequences:

$$S_\beta = \frac{\beta}{\theta_i} \frac{\partial U}{\partial \beta} \quad (22)$$

Sensitivity coefficients show that during the first microseconds, temperature variation is very sensitive to the thermal diffusivity of clad layer, and progressively more to the substrate one (Fig. 7). From about 50 up to 500 μs, substrate thermal diffusivity is the only one sensitive parameter. Sensitivity coefficients on R_c (Fig. 8) makes appear at high sensitivity to R_c beyond several milliseconds. It means that R_c determines strongly temperature levels, but does not affect transient state before about 1 μs.

In conclusion of this theoretical study, transient state is very sensitive to clad layer N-GaAlAs properties up to 10^{-6} s. From about 50 μs, transient response is equivalent to a perfectly homogeneous laser having a single junction of B_0 width. During the sequence [50, 100 μs], substrate diffusivity α is the only one parameter occurring in the expression of T^*, α may be then identified. After a few milliseconds, temperature distribution become monodimensional inside the laser and T^* depends simultaneously on R_c and α. R_c can be estimated directly because α has been identified in the previous sequence. The sequence 3–4 ms is very sensitive to R_c.

6. EXPERIMENTAL ARRANGEMENT

The experimental arrangement is shown in Fig. 9. The laser diode [3] is driven, in a primary circuit, by a pulse generator [1]. Measurement of current intensity I is achieved from a standard resistor R [2] = 1 Ω. This circuit can be switched off, on a measurement circuit, driven by a battery [5], supplying the current I_0. The intensity of I_0 is fixed from a resistor R' [4] of a few hundreds of ohms. A silicon diode [6], reverse

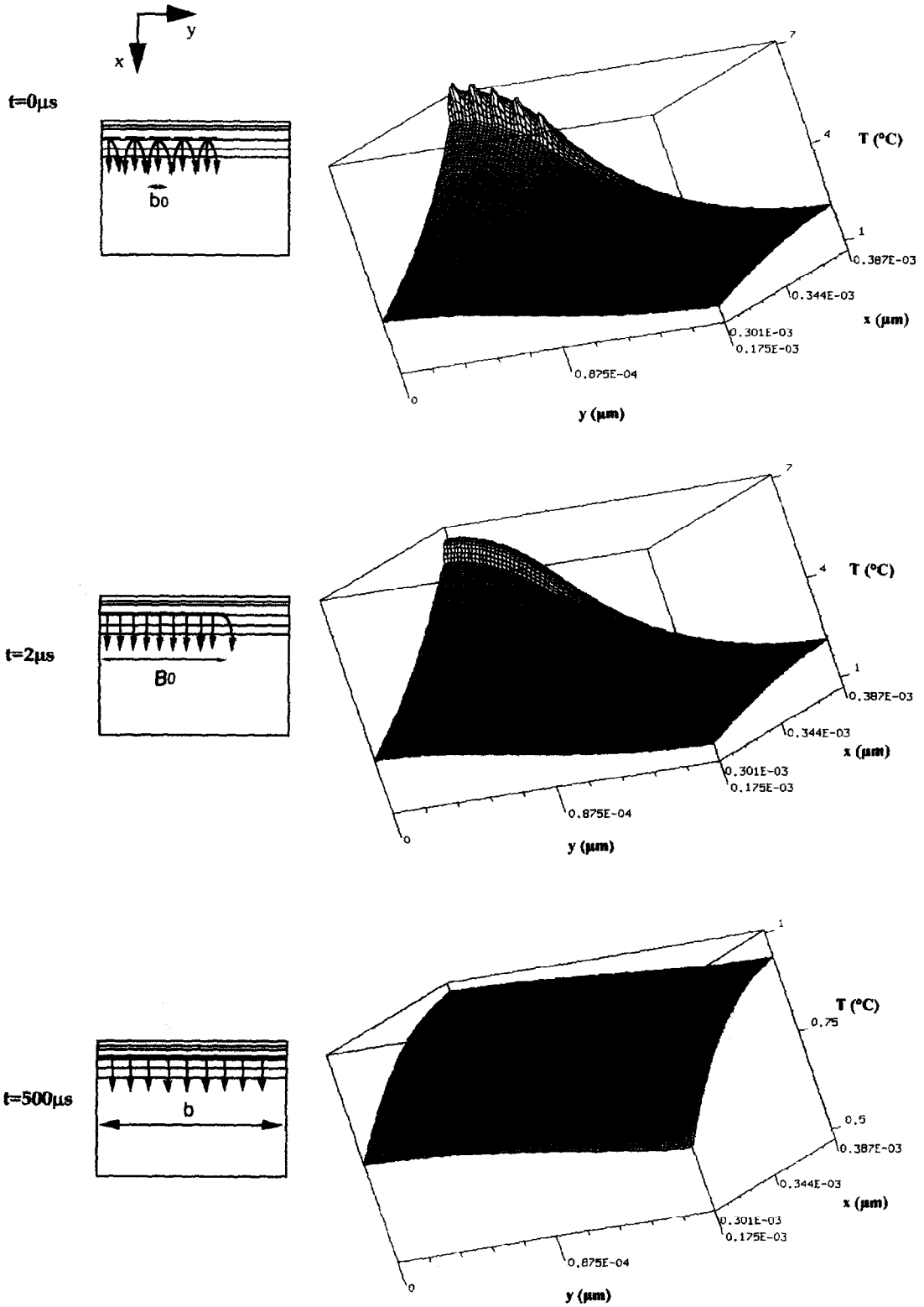

Fig. 4. Temperature fields ($P = 0.25$ W, $R_c = 10^{-6}$ K m^2/W, $T_a = 0$°C).

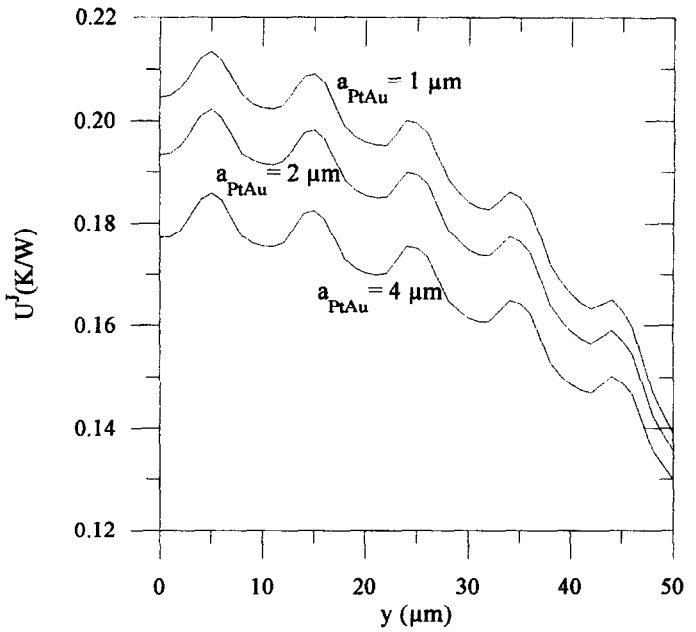

Fig. 5. Temperature profiles as a function of metallization thickness, in steady state.

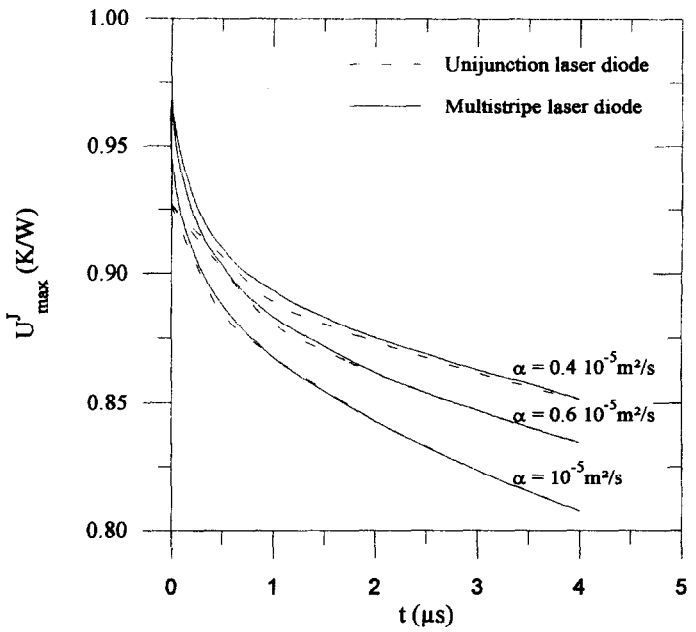

Fig. 6. Compared cooling down behaviours.

biased after switching off, insulates the laser diode during the measurement sequence from the primary circuit. I_0 must be sufficiently high to work under an acceptable impedance of the diode. In this way, noises and capacity effects are reduced.

The laser diode [3] is set in an isothermal cell, controlled by a thermostated water flow. The insulated moving part prevents convective transfer, and the water flow imposes a constant temperature under the submount. Temperature is tested by several K thermocouples (80 μm). A thermocouple (25 μm) has been fixed at the back of the submount (Fig. 10).

Junction temperature is obtained, measuring the terminal voltage $\delta V(\theta)$ across the diode by means of a digital transient recorder (analog bandwidth of 25 MHz, input impedance of 1 MΩ). An offset circuit [7], composed of a battery and a resistor, removes δV of about 0.8 V. This tension corresponds approximately to δV at steady state temperature with a current I_0. Detection is then performed at highest res-

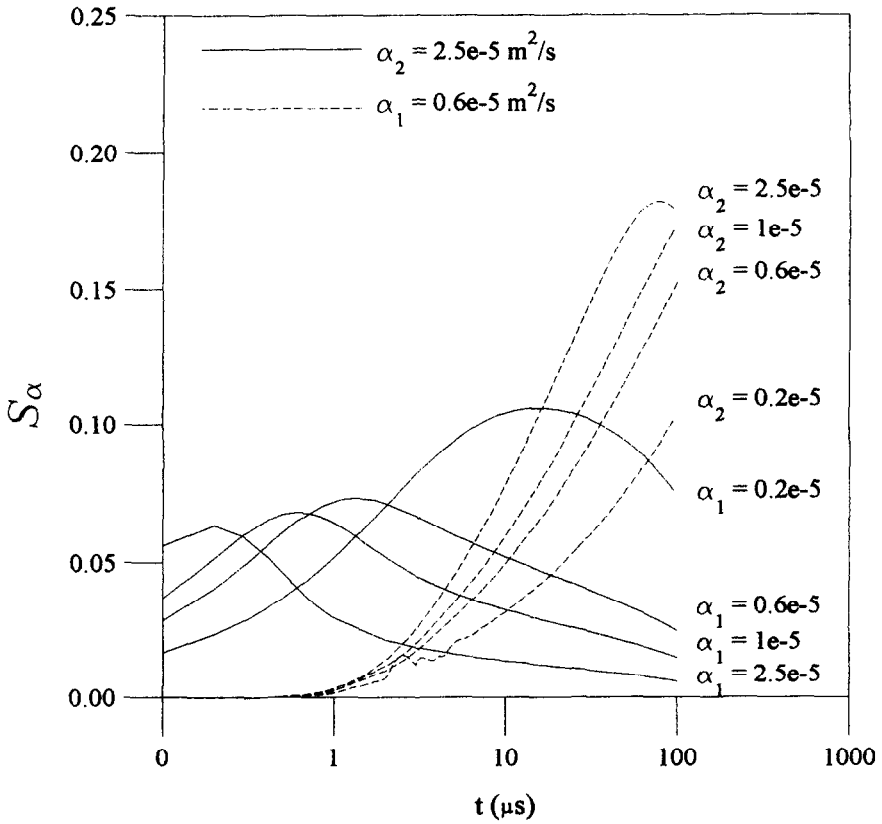

Fig. 7. Sensitivity coefficients on diffusivities indexes 1: clad layer—2: substrate.

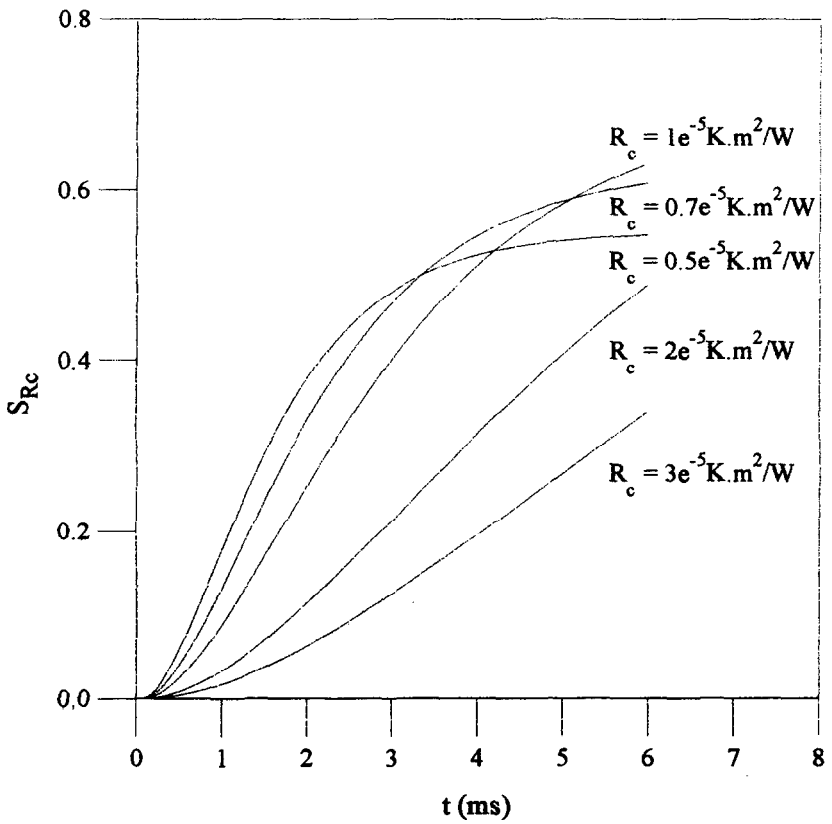

Fig. 8. Sensitivity coefficients on thermal contact resistance.

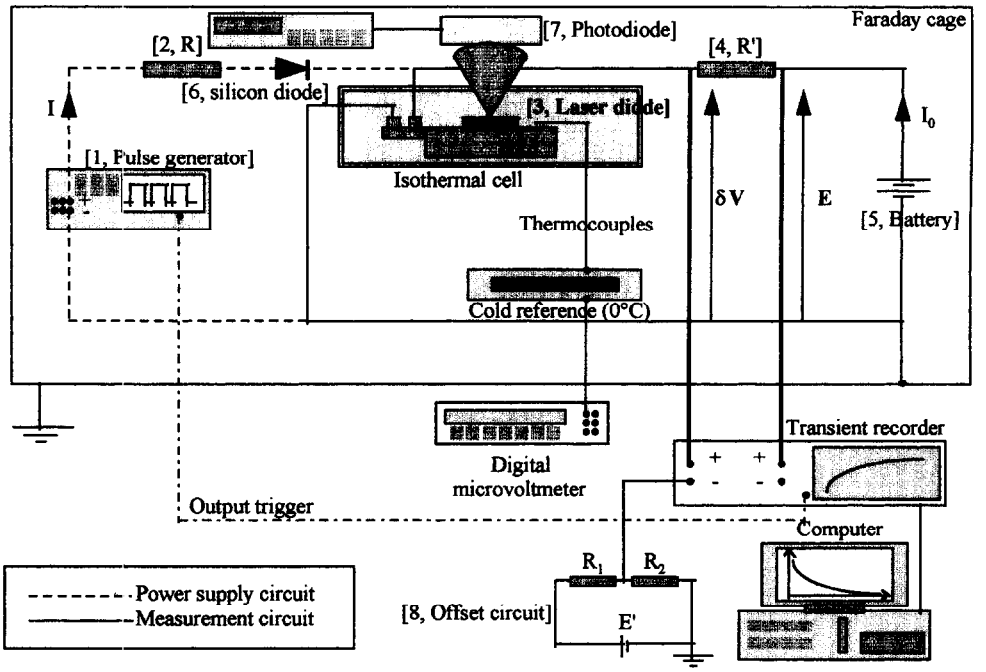

Fig. 9. Experimental arrangement.

Table 3. N-GaAs diffusivity, thermal resistance of the adhesive bond and for various input power ($T_a = 20.6$°C). Interval [70, 80 μs] for α and [3, 3.8 ms] for R_c

I (mA)	α (m^2/s)	I (mA)	R_c (K m^2/W)
189	2.58×10^{-5}	179	1.61×10^{-5}
178	2.46×10^{-5}	204	1.52×10^{-5}
172	2.72×10^{-5}		

Table 4. N-GaAs thermal diffusivity, thermal contact resistance obtained on various sequence ($I = 178$ mA)

Interval (μs)	α (m^2/s)	Interval (ms)	R_c (K m^2/W)
70–75	2.50×10^{-5}	3–3.5	1.60×10^{-5}
70–80	2.46×10^{-5}	3–3.6	1.61×10^{-5}
70–85	2.45×10^{-5}	3–3.8	1.61×10^{-5}
70–90	2.43×10^{-5}	3–4	1.62×10^{-5}

olution of the detection system (full scale 100 mV, resolution 100 μV).

δV is composed of a potential barrier, at the junction, and a thermoelectric voltage due to non-uniformity of temperature distribution (Seebeck effect). These two contributions may be taken as linear functions of temperature [12, 14, 15]. Temperature measurement requires, on one part a calibration during which δV is measured, in isothermal conditions, in function of the junction temperature with a current I_0. So, this calibration gives the contribution of the potential barrier. The sensitivity of potential barrier towards temperature, at $I_0 = 1$ mA, is about -3 mV/°C. On the other part, the contribution of thermoelectric voltage is practically identical to substrate thermoelectric power (0.2 mV/°C), and represents about 10% of junction barrier effect.

7. EXPERIMENTAL RESULTS

Experiments has been performed on a conventional double heterostructure GaAlAs laser having ten stripes. Pulse generator frequency was 0.1 Hz, with a duty cycle of 99% (pulse width = 9.9 s). Currents were from 100 to 300 mA under a voltage of about 1.5 V. Input power was from 0.1 W to 0.5 W. Output

Table 5. Experimental and theoretical cooling down

t (μs)	θ (°C)	T (°C)	$(T-\theta)/\theta$ (%)
5	38.2	38.7	1.3
10	37.8	38.3	1.3
20	37.1	37.7	1.6
30	36.6	37.0	1.2
40	36.1	36.7	1.7
50	35.7	36.3	1.6
70	35.2	35.7	1.4
80	35.0	35.5	1.4
90	34.8	35.3	1.4
100	34.6	35.1	1.4
2000	27.3	27.2	−0.2
2500	27.1	26.9	−0.9
3000	27.1	26.7	−1.3

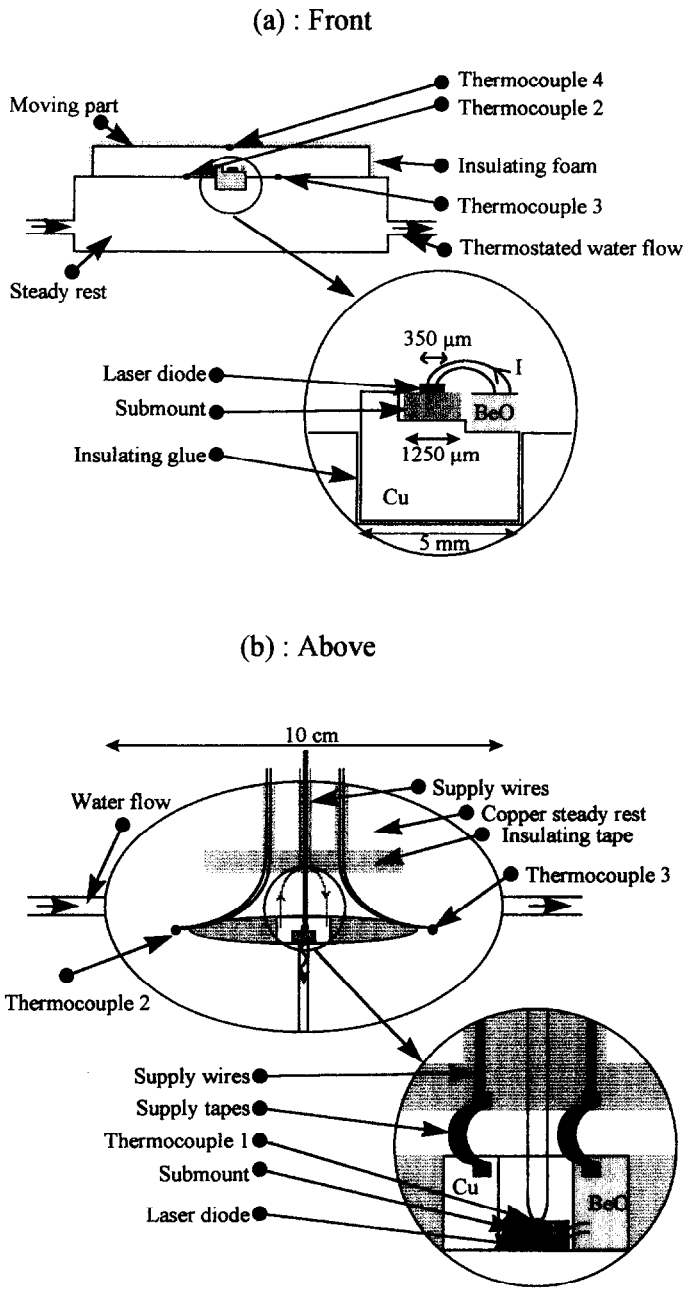

Fig. 10. Instrumentation and thermocouples location.

optical power was included between 0 to 0.1 W. The measurement current I_0 was chosen at ~ 1 mA. Figure 11 presents experimental temperature evolution for 500 μs under several input powers. It appears that temperature rise is roughly a linear function of input power (Fig. 12). It means that optical efficiency is poorly sensitive to the temperature.

N-GaAs diffusivity and thermal contact resistance have been identified from relation (6). Properties of other laser diode layers and submount are taken equal to those of Table 1. N-GaAs substrate diffusivity α has been identified on the sequence [50–100 μs]. The thermal contact resistance R_c has been identified on the sequence [3–4 ms]. A thermal diffusivity $\alpha = 2.59 \times 10^{-5}$ m^2/s and a thermal contact resistance $R_c = 1.55 \times 10^{-5}$ K m^2/W have been obtained (Table 3). Identification on other intervals and currents gives also acceptable results (Table 4). A very good agreement is observed between experimental and theoretical temperatures from 10^{-5} up to 10^{-3} (Table 5). Relative difference appears less than 2%. These results show that thermophysical properties are poorly dependent of the temperature. The thermal diffusivity is very closed to the value proposed in [7]. An esti-

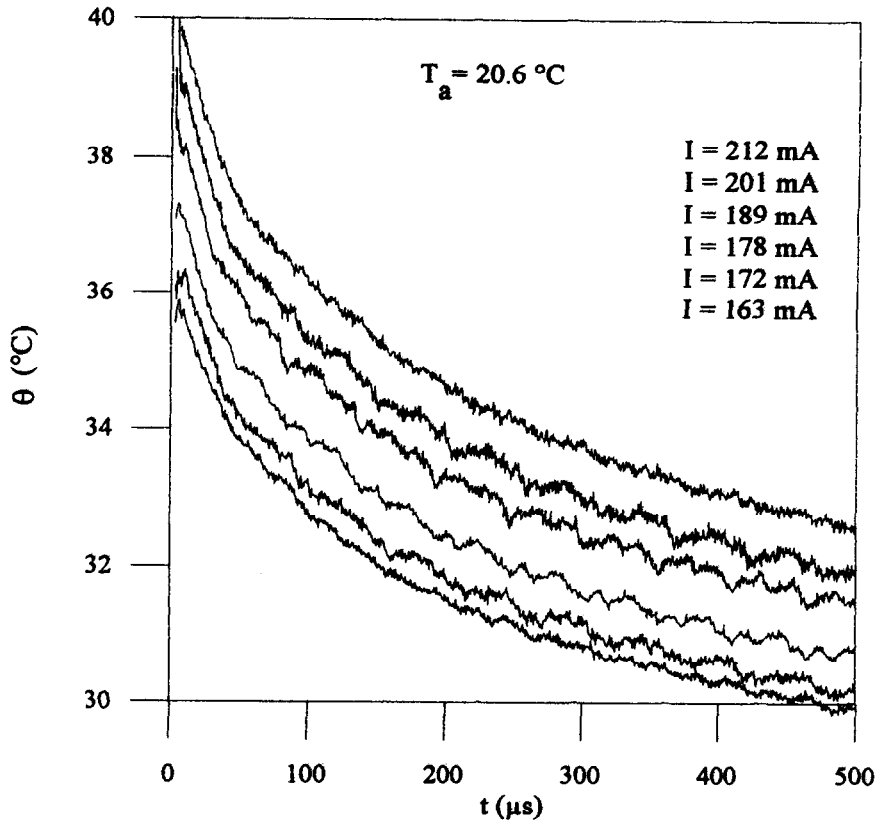

Fig. 11. Experimental temperature decreasing.

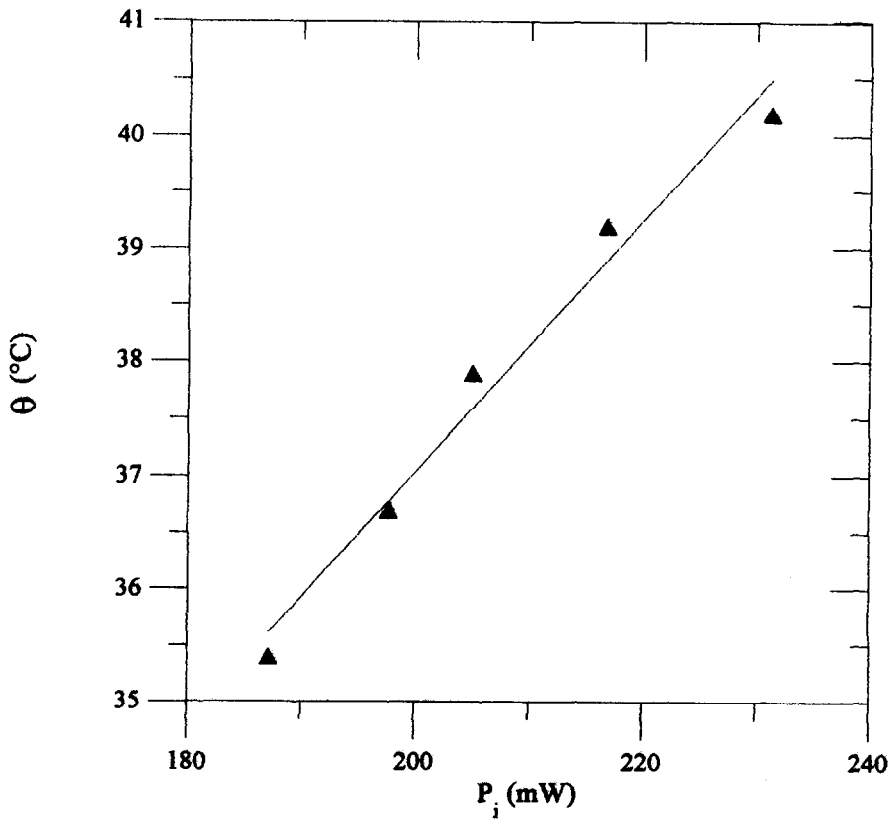

Fig. 12. Steady state temperature versus input power.

Table 6. Values of θ_i, P, η identified at different times, for $I = 172$ mA

t (μs)	θ_i (°C)	P (mW)	η
80	36.7	125.8	0.36
90	36.7	125.7	0.36
100	37.7	125.6	0.36

Table 7. Values of θ_i, P, η identified with various currents, at $t = 80$ μs

Current (mA)	Input power P_i (mW)	Dissipated power P (mW)	η	θ_i (°C)
201.3	231	168.3	0.27	40.2
188.9	217	164.1	0.24	39.2
178.4	205	148.1	0.27	37.9
172.2	198	125.9	0.36	36.7
162.9	187	95.2	0.49	35.4

mation of specific heat and density ($Cp = 334.4$ J/kg K, $\rho = 5360$ kg/m^3) leads to a thermal conductivity $\lambda = 46.4$ W/m K.

Precision are estimated of $\sim 5\%$ for the thermal diffusivity and 10% for the thermal contact resistance. Thermophysical properties of clad layer $Al_xGa_{1-x}As$ given by Adachi [7] have been taken for the determination of $\theta_i P$, η (calculation of U in relations (7)–(9)). Results are in Tables 6 and 7.

It has to be noticed that efficiency above real value is identified for low input current (≈ 187 mW). In this range, current is near threshold and spontaneous emission process is important [2–5]. Radiative transfer due to photon absorption in N-GaAs and P-GaAs layers cannot still be neglected. The consequence is that heat generation rate is not only located at junctions, an identification model has to take into account radiative transfer. Other levels, which correspond to usual operating conditions ($P_i > 200$ mW), give coherent results.

8. CONCLUSION

A method to measure the thermal diffusivity of laser diodes simultaneously with thermal resistance of their adhesive joints has been set up. This method is based on analysis of temperature variations of emitting zones caused by a quasi-continuous heat generation. A constant input power is applied in the laser diode during several seconds, and switched off during some milliseconds. Temperature variations are detected during sequences from 10^{-6} to 10^{-3} s. They are obtained from terminal voltage measurements resulting from injection of a small current. Parameter identification used a multidimensional heat diffusion model based on integral transform. Results are obtained on a multistripe double heterostructure GaAs/GaAlAs laser diode owning ten emitting zones of 4 μm width. Thermal diffusivity of the substrate (N-GaAs) and thermal resistance of its adhesive joint have been identified. In addition, this method allows one to estimate steady state junction temperature and optical output power as a function of current intensity. This method can be used for failure analysis and constitutes a useful tool for non-destructive tests and thermal characterization of laser diodes.

REFERENCES

1. Casey, H. C. and Panish, M. B., *Heterostructure Lasers*. Academic Press, 1978.
2. Bertolotti, M. *et al.*, *Appl. Phys. Lett.*, 1994, **65**, 2266–2268.
3. Blakemore, J. S., *J. Appl. Phys.*, 1982, **53**, R123–R181.
4. Chen, G. *et al.*, *J. of Heat Transfer*, 1994, **116**, 325–331.
5. Drenten, R. R. *et al.*, *J. Appl. Phys.*, 1994, **76**, 3988–3993.
6. Bardon, J. P., *Eurotherm Proceedings No.* 4. Nancy, 1988, pp. 40–74.
7. Adachi, S., *J. Appl. Phys.*, 1985, **58**, R1–R29.
8. Joyce, W. B. and Dixon, R. W., *J. Appl. Phys.*, 1975, **48**, 855–682.
9. Kobayashi, T. and Furukawa, Y., *Japanese J. Appl. Phys.*, 1975, **14**, 1981–1986.
10. Steventon, A. G. *et al.*, *Opt. Quant. Electr.*, 1977, **9**, 519–525.
11. Osizik, N. M., *Heat Conduction*, John Wiley and Sons, 1993.
12. Lepaludier, V., Ph.D. thesis, University of Nantes, France, 1995.
13. Stehfest Gaver, H., *Commun. ACM*, 1970, **13**, 47–49.
14. Lepaludier, V. and Scudeller, Y., *Eurotherm No.* 45, Leuven, Belgium, September 1995.
15. Lepaludier, V. and Scudeller, Y., *Microelectronics Journal*, 1997, **28**, 301–312.

APPENDIX

In Fourier–Laplace space, conduction system in the laser diode is written:

$$\begin{cases} \dfrac{d^2\tilde{\tilde{U}}_i}{dx_i^2} - \xi_m^2 \cdot \tilde{\tilde{U}}_i = 0 \quad \text{with } \xi_m^2 = \dfrac{\lambda_y^i}{\lambda_x^i}\alpha_m^2 + \dfrac{\rho_i C_i}{\lambda_x^i} p \\ x_1 = 0 \quad \dfrac{d\tilde{\tilde{U}}_1}{dx_1} = 0 \\ x_i = 0 \quad \begin{cases} \tilde{\tilde{U}}_i(x_i = 0) = \tilde{\tilde{U}}_{i-1}(x_{i-1} = a_{i-1}) \\ \lambda_x^i \dfrac{d\tilde{\tilde{U}}_i}{dx_i}(x_i = 0) = \lambda_x^{i-1} \dfrac{d\tilde{\tilde{U}}_{i-1}}{dx_{i-1}}(x_{i-1} = a_{i-1}) \end{cases} \\ x_i = a_i \quad \begin{cases} \tilde{\tilde{U}}_i(x_i = a_i) = \tilde{\tilde{U}}_{i+1}(x_{i+1} = 0) \\ \lambda_x^i \dfrac{d\tilde{\tilde{U}}_i}{dx_i}(x_i = a_i) = \lambda_x^{i+1} \dfrac{d\tilde{\tilde{U}}_{i+1}}{dx_{i+1}}(x_{i+1} = 0) \end{cases} \\ x_{J+1} = 0 \quad \begin{cases} \tilde{\tilde{U}}_{J+1}(x_{J+1} = 0) = \tilde{\tilde{U}}_J(x_J = a_J) \\ -\lambda_x^{J+1} \dfrac{d\tilde{\tilde{U}}_{J+1}}{dx_{J+1}}(x_{J+1} = 0) = -\lambda_x^J \dfrac{d\tilde{\tilde{U}}_J}{dx_J}(x_J = a_J) + \tilde{\tilde{q}} \end{cases} \\ x_N = a_N \quad \tilde{\tilde{U}}_N = (\tilde{\tilde{F}}(p) + R_c) \cdot \tilde{\tilde{q}}_c \end{cases} \tag{A1}$$

Temperature and flux at interface i are written as functions of temperature and flux at interface $i-1$, by means of a transfer matrix M_i:

$$\begin{pmatrix} \tilde{\tilde{U}}_i \\ \tilde{\tilde{q}}_i \end{pmatrix}_{x_i = a_i} = M_i \begin{pmatrix} \tilde{\tilde{U}}_{i-1} \\ \tilde{\tilde{q}}_{i-1} \end{pmatrix}_{x_{i-1} = a_{i-1}}$$

$$\text{with } M_i = \begin{pmatrix} \operatorname{ch}(\xi_m a_i) & -\dfrac{\operatorname{sh}(\xi_m a_i)}{\xi_m \cdot \lambda_x^i} \\ \xi_m \cdot \lambda_x^i \cdot \operatorname{sh}(\xi_m a_i) & \operatorname{ch}(\xi_m a_i) \end{pmatrix} \tag{A2}$$

Temperature field is obtained writing temperature and flux at $x_N = a_N$ as a function of temperature and flux at $x_1 = 0$:

$$\begin{pmatrix} \tilde{\tilde{U}}_N \\ \tilde{\tilde{q}}_N \end{pmatrix}_{x_N = a_N} = M_N \cdot M_{N-1} \ldots M_i \ldots M_1 \begin{pmatrix} \tilde{\tilde{U}}_1 \\ 0 \end{pmatrix}_{x_1 = 0} + M_N \cdot M_{N-1} \ldots M_{J+1} \begin{pmatrix} 0 \\ \tilde{\tilde{q}} \end{pmatrix}_{x_J = a_J} \tag{A3}$$

Moreover, considering relation (17), we obtain:

$$\begin{pmatrix} \tilde{\tilde{T}}_c \\ \tilde{\tilde{q}}_c \end{pmatrix} = \begin{pmatrix} \tilde{\tilde{T}}_c \\ \tilde{\tilde{T}}_c \\ \hline \tilde{\tilde{F}} \end{pmatrix} = R \begin{pmatrix} \tilde{\tilde{U}}_N \\ \tilde{\tilde{q}}_N \end{pmatrix}_{x_N = a_N} \quad \text{with } R = \begin{pmatrix} 1 & -R_c \\ 0 & 1 \end{pmatrix} \tag{A4}$$

So, $\tilde{F}$ being expression (relation 18), $\tilde{\tilde{T}}_c$ and $\tilde{\tilde{U}}_1$ can be determined with both equations:

$$\begin{pmatrix} \tilde{\tilde{T}}_c \\ \tilde{\tilde{q}}_c \end{pmatrix} = \begin{pmatrix} \tilde{\tilde{T}}_c \\ \tilde{\tilde{T}}_c \\ \hline \tilde{\tilde{F}} \end{pmatrix} = R \cdot \left[\prod_{k=N}^{1} M_k \cdot \begin{pmatrix} \tilde{\tilde{U}}_1 \\ 0 \end{pmatrix} + \prod_{k=N}^{J+1} M_k \cdot \begin{pmatrix} 0 \\ \tilde{\tilde{q}} \end{pmatrix} \right] \tag{A5}$$

All boundary conditions being known, temperature and flux can be expressed at each interface of the laser diode:

$$i \leqslant J \quad \begin{pmatrix} \tilde{\tilde{U}}_i \\ \tilde{\tilde{q}}_i \end{pmatrix}_{x_i = a_i} = \prod_{k=i}^{1} M_k \begin{pmatrix} \tilde{\tilde{U}}_1 \\ 0 \end{pmatrix}_{x_1 = 0}$$

$$i > J \quad \begin{pmatrix} \tilde{\tilde{U}}_i \\ \tilde{\tilde{q}}_i \end{pmatrix}_{x_i = a_i} = \prod_{k=i}^{1} M_k \begin{pmatrix} \tilde{\tilde{U}}_1 \\ 0 \end{pmatrix}_{x_1 = 0} + \prod_{k=i}^{J+1} M_k \begin{pmatrix} 0 \\ \tilde{\tilde{q}} \end{pmatrix}_{x_{J+1} = 0} \tag{A6}$$